# Chapter 5

# Graded-index fibers (GRA)

This chapter describes the wave propagation in graded-index fibers. In particular, the number of propagable waves and the optimal shape of the refractive index profile will be discussed.

The single-mode step-index fiber has a high bandwidth (essentially limited only by the waveguide dispersion and material), but has, due to the generally small fiber parameter $V$, either a small core diameter or a small numerical aperture. This leads to problems with linking such fibers. Presuming multi-mode step-index fibers (high $V$) the eigenmodes have in general different propagation delays, resulting in a pulse broadening (see Hochfrequenztechnik I for further details). Thus:

$$\Delta t \approx \frac{N_1 L}{2 \cdot c \cdot n_1^2} A_N^2 \tag{5.1}$$

$N_1$ denotes the group index in the fiber core and $L$ is the fiber length. This limits the transmission rate to approximately 20 to 100 Mbit/s based on 1 km of fiber length.
For these reasons, searching for a refractive index profile in which all the eigenmodes have nearly the same running time is necessary. The so-called graded-index fiber is a possible solution.

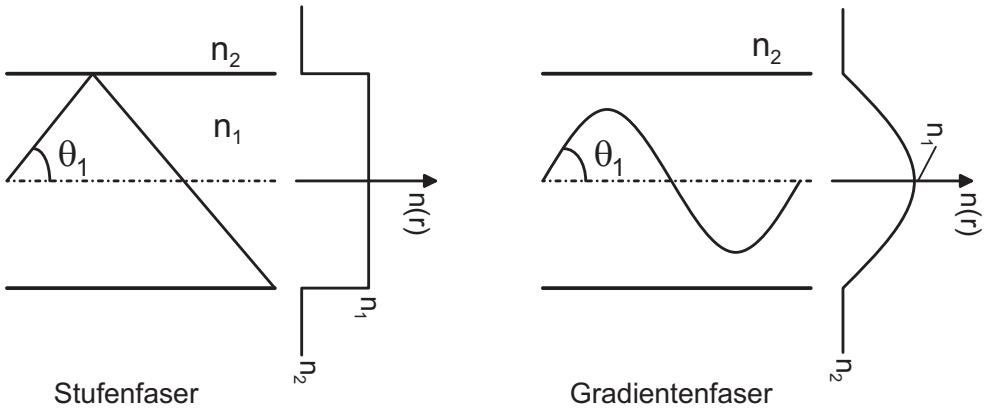


Figure 5.1: Motivation for a graded-index fiber in a beam optical illustration

For waves with a higher $\theta_1$, the distance covered by the beam increases. Thus, in the step-index fiber, the

transit time is increases. In the graded-index fiber the rays with higher $\theta_1$ reach into regions with a lower refractive index. Hence they are faster. By suitable choice of a refractive index profile $n(r)$ these two effects can cancel each other out.

## 5.1 Field calculation

For linearly polarized waves in graded-index fibers the scalar wave equation

$$\triangle \underline{E}_{x,y} + k_0^2 n^2(r) \underline{E}_{x,y} = 0 \tag{5.2}$$

is effective. Firstly an $x$-direction linearly polarized wave of the form

$$\underline{E}_x = \psi(r, \varphi) \exp(-j\beta z) \tag{5.3}$$

is assumed. Therefore the scalar wave equation for $\psi(r, \varphi)$ results in:

$$\triangle_t \psi + \left(k_0^2 n^2(r) - \beta^2\right) \psi = 0 \tag{5.4}$$

in cylindrical coordinate this yields

$$\frac{1}{r}\frac{\partial}{\partial r}\left(r \cdot \frac{\partial \psi}{\partial r}\right) + \frac{1}{r^2}\frac{\partial^2 \psi}{\partial \varphi^2} + \left(k_0^2 n^2(r) - \beta^2\right) \psi = 0 \tag{5.5}$$

In contrast to step-index fibers, the refractive index $n(r)$ is now dependent on the radial coordinate $r$.
For a $\mathrm{LP}_{lp}$-wave with the circumferential order $l$ for $\psi(r, \varphi)$ the result is:

$$\psi(r, \varphi) = \psi_r(r) \left\{ \begin{array}{c} \cos(l \cdot \varphi) \\ \sin(l \cdot \varphi) \end{array} \right\} \tag{5.6}$$

Inserting this approach into the wave equation (5.5), the radial field variable $\psi_r(r)$ can be obtained:

$$\frac{1}{r}\frac{\mathrm{d}}{\mathrm{d}r}\left(r \frac{\mathrm{d}\psi_r(r)}{\mathrm{d}r}\right) + \underbrace{\left(k_0^2 n^2(r) - \beta^2 - \frac{l^2}{r^2}\right)}_{k_r^2} \psi_r(r) = 0. \tag{5.7}$$

Therefore

$$k_r = \sqrt{k_0^2 n^2(r) - \beta^2 - \frac{l^2}{r^2}} \tag{5.8}$$

can be interpreted as wave number in radial direction (fig. 5.2). The zeros of $k_r^2$ are $r_1$ and $r_2$, which are called the inner and outer turning radius.

| | | |
|---|---|---|
| $k_r$ | -is real for $r_1 < r < r_2$ | $\Rightarrow \psi$ oscillating |
| $k_r$ | -is imaginary for $r < r_1$ or $r > r_2$ | $\Rightarrow \psi$ decays exponentially |

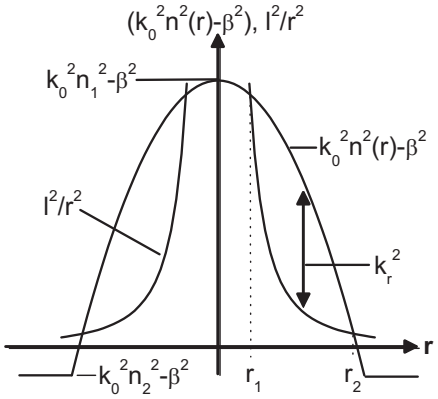


Figure 5.2: Schematic of the wave number in radial direction $k_r$ and the turning radius $r_1$ and $r_2$

Thus, the field is concentrated in the region between $r_1$ and $r_2$.
In order to avoid the singularities at $r = 0$ in (5.7), the substitution $r = a \cdot \exp(w)$ is applied. Then the wave equation is given by:

$$\frac{\mathrm{d}^2\psi_r}{\mathrm{d}w^2} + Q_w^2\psi_r = 0 \tag{5.9}$$

with $Q_w^2 = r^2 \cdot k_r^2$.
It is $Q_w^2 = 0$ for $w_1$ and $w_2$. Thus $r_1 = a\exp(w_1)$ and $r_2 = a\exp(w_2)$ apply,
as long as $|Q_w|$ is sufficiently large and is only weakly dependent of $w$ ($r$ respectively), eq. (5.9) is approximately solved by the *WKB-solution* (Wentzel, Kramers, Brillouin):

$$\psi_r \approx \frac{A}{\sqrt{Q_w}} \exp\left(\pm j \int Q_w dw\right) \tag{5.10}$$

As long as $Q_w \neq 0$ applies, three cases are apply:

1. $w < w_1 \quad \Rightarrow \quad Q_w^2, k_r^2 < 0$

$$\psi_r \approx \frac{A}{\sqrt{|Q_w|}} \exp\left(-\int_w^{w_1} |Q_w| \ \mathrm{d}w\right) \tag{5.11}$$

2. $w_1 < w < w_2 \quad \Rightarrow \quad Q_w^2, k_r^2 > 0$

$$\psi_r \approx \frac{B}{\sqrt{Q_w}} \cos\left(\int_{w_1}^{w} Q_w \ \mathrm{d}w + \theta\right) \tag{5.12}$$

3. $w > w_2 \quad \Rightarrow \quad Q_w^2, k_r^2 < 0$

$$\psi_r \approx \frac{C}{\sqrt{|Q_w|}} \exp\left(-\int_{w_2}^{w} |Q_w| \ \mathrm{d}w\right) , \tag{5.13}$$

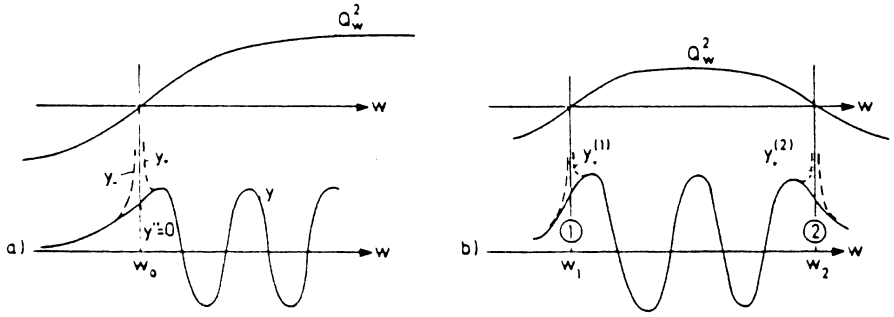


Figure 5.3: WKB-solution for the problem (a) with one turning point and (b) with two turning points (Illustration taken from: Timmermann, Lichtwellenleiter)

where $A$, $B$ and $C$ in eq. (5.11), eq. (5.12) and eq. (5.13) designate constants. In order for eq. (5.11) and eq. (5.12), as well as eq. (5.12) and eq. (5.13) to be continuously differentiale at $w \approx w_1$, and $w \approx w_2$, respectively, it follows from fig. 5.3, that for $w \to w_1$ the argument of the cosine in eq. (5.12) must take the value $-\frac{\pi}{4}$ and for $w \to w_2$ the value $m \cdot \pi + \frac{\pi}{4}$ ($m$ - of integer). These intuitive considerations are confirmed by accurate calculations. In addition, $A = C = \frac{B}{2}$ (see Flügge, Rechenmethoden der Quantentheorie, Springer, Berlin-Heidelberg 1965, S.159)
Therefore the result is given by

$$\theta = -\frac{\pi}{4} \quad \text{and} \quad \int_{w_1}^{w_2} Q_w \, \mathrm{d}w = \left(m + \frac{1}{2}\right)\pi = \left(p - \frac{1}{2}\right)\pi \tag{5.14}$$

with the radial modal number $p = 1, 2, 3...$ of the $\mathrm{LP}_{lp}$-wave. With the relation $\mathrm{d}r = r \cdot \mathrm{d}w$, eq. (5.14) can be determined as:

$$\int_{r_1}^{r_2} k_r dr = \left(p - \frac{1}{2}\right)\pi \tag{5.15}$$

Because of the approximation in eq. (5.10), the equations (5.14) and (5.15) only apply for $p \gg 1$.
For particular $\mathrm{LP}_{lp}$-waves the propagation constant $\beta$ can be determined from eq. (5.15). If $l$ and $p$ are given, $\beta$ has to be chosen to satisfy (5.15) (in general only numerically feasible).

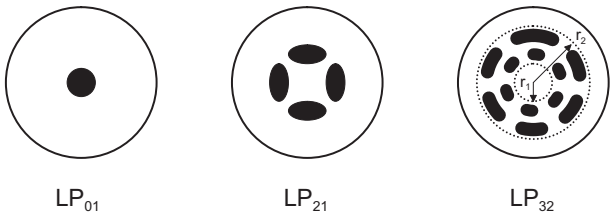


Figure 5.4: Field representation of the $\mathrm{LP}_{lp}$-waves

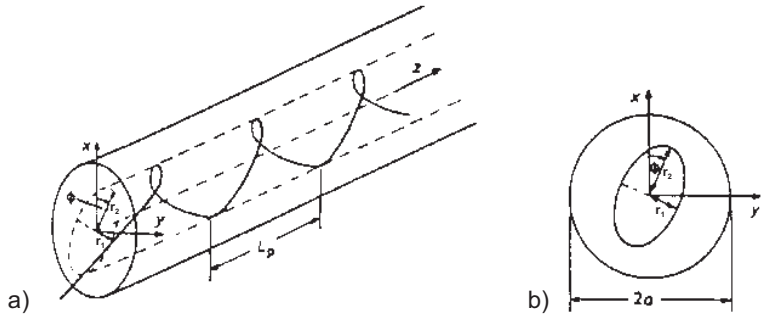


Figure 5.5: (a) Spiral-shaped beam path in a graded-index fiber with a parabolic refractive index profile, (b) cross-section projection of a beam path (Illustration taken from: Unger, Optische Nachrichtentechnik I)

## 5.2 Number of propagable Modes

For modal number combination ($l$,$p$) there are:
2 modes for $l = 0$ (2 polarizations)
4 modes for $l \neq 0$ (2 polarizations and 2 orientations, $\sin(l \cdot \varphi)$ and $\cos(l \cdot \varphi)$)

A refractive index profile $n(r)$ is given, that declines monotonously for a rising $r$ ( $r < a$ ) and that remains constant $n(r) = n_2$ for $r \geq a$. To answer the question of the number of guided modes and therefore the modal number of combinations ($l$, $p$), eq. (5.15) is evaluated. Eq. (5.8) and eq. (5.15) result in

$$\left(m + \frac{1}{2}\right)\pi = \int_{r_1}^{r_2} \sqrt{k_0^2 \cdot n^2(r) - \beta^2 - \frac{l^2}{r^2}}\ \mathrm{d}r \tag{5.16}$$

with the radial modal numbers $m = (p-1)$ ( $m = 0, 1, 2, ...$ ).
Assuming a waveguide with large number of guided modes, eq. (5.16) can be approached by:

$$m \cdot \pi \approx \int_{r_1}^{r_2} \sqrt{k_0^2 \cdot n^2(r) - \beta^2 - \frac{l^2}{r^2}}\ \mathrm{d}r \tag{5.17}$$

The maximum radial modal or order number $m = m_{max}$ is reached for $\beta = k_0 n_2$ with a given $l$. Thus:

$$m_{max} \cdot \pi \approx \int_{r_1}^{r_2} \sqrt{k_0^2 \cdot \left(n^2(r) - n_2^2\right) - \frac{l^2}{r^2}}\ \mathrm{d}r \tag{5.18}$$

In this equation $r_1$ and $r_2$ are the turning radii for $\beta = k_0 n_2$. Then the total number of modes $M$ can be calculated by:

$$M \approx 4 \cdot \sum_{l=0}^{l_{max}} m_{max}(l) \approx 4 \cdot \int_{0}^{l_{max}} m_{max}(l) dl \tag{5.19}$$

The factor 4 follows from the four possible modes for a given modal number combination $(l, p)$, where $l \neq 0$. Inserting $m_{max}$ from eq. (5.18), therefore:

$$M \approx \frac{4}{\pi} \cdot \int_0^{l_{max}} \int_{r_1}^{r_2} \sqrt{k_0^2 \cdot \left(n^2(r) - n_2^2\right) - \frac{l^2}{r^2}} \; \mathrm{d}r \; \mathrm{d}l \tag{5.20}$$

In eq. (5.20) the integration proceed firstly over $r$ and afterwards over $l$ (Integration limits shown in fig.

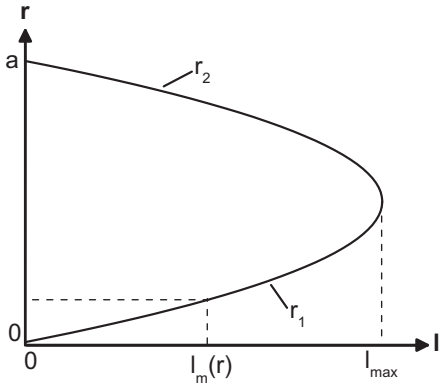


Figure 5.6: Representation of the integration limits in the $r$, $l$-plane

5.6). The order is reversed to simplify the integration:

$$M \approx \frac{4}{\pi} \cdot \int_0^{a} \int_{0}^{l_m(r)} \sqrt{k_0^2 \cdot \left(n^2(r) - n_2^2\right) - \frac{l^2}{r^2}} \; \mathrm{d}l \; \mathrm{d}r \tag{5.21}$$

The radial order $l_m(r)$ is given by the fact, that for $l = l_m(r)$ the radial wave number results in $k_r^2 = k_0^2 \cdot (n^2(r) - n_2^2) - l^2/r^2 = 0$.

$$\Rightarrow \quad l_m(r) = r \cdot k_0 \sqrt{n^2(r) - n_2^2} \tag{5.22}$$

Therefore, after the integration over $l$:

$$M = k_0^2 \cdot \int_0^{a} \left(n^2(r) - n_2^2\right) r \; \mathrm{d}r \tag{5.23}$$

The number of guided modes is proportional to the rotation volume, which is formed by the refractive index profile.

1. Example: parabolic refractive index profile

$$n^2(r) = \begin{cases} n_1^2 \cdot \left(1 - 2\Delta \cdot \dfrac{r^2}{a^2}\right) & \text{for } r \leq a \\ n_1^2 \cdot (1 - 2\Delta) = n_2^2 & \text{for } r > a \end{cases} \tag{5.24}$$

$\Delta$ represents the relative refractive number difference: $\Delta = \frac{n_1^2 - n_2^2}{2n_1^2} \approx \frac{n_1 - n_2}{n_1}$
In this case, the number of modes is given by:

$$M = \frac{V^2}{4} \tag{5.25}$$

with $V = a \cdot k_0 \cdot \sqrt{n_1^2 - n_2^2} = a \cdot k_0 \cdot n_1 \cdot \sqrt{2\Delta}$

2. Example: Step-index fiber

$$n^2(r) = \begin{cases} n_1^2 & \text{for } r \leq a \\ n_2^2 & \text{for } r > a \end{cases} \tag{5.26}$$

In this case the number of modes is:

$$M = \frac{V^2}{2} \tag{5.27}$$

For a typical multi-mode optical fiber with $2a = 50\,\mu\text{m}$, $n_1 = 1.45$, $\Delta = 0.01$, $A_N = 0.205$ and $\lambda = 1.3\,\mu\text{m}$ there are approximately 152 modes guided in a parabolic refractive profile and 306 propagable modes for a step-index profile.
The detailed analysis in section STU, fig. 6 provides, for example, for $V = 6$ and $V = 8$, 20 and 34 propagable modes, respectively, while the approximation eq. (5.27) leads to 18 and 32 propagable modes, which is, in the context of the used approximations means, a good accordance.

## 5.3 Propagation delay between the eigenmodes

### 5.3.1 Profile dispersion

The aim of the following calculations is to determine a refractive index profile in which all the modes have almost the same propagation delay. According to the optical beam model, the path of a beam belonging to a wave is determined through the refractive index profile $n(r)$ and the propagation delay of the wave along the beam path is described by the group index $N(r)$. Thus the delay depends obviously on both the refractive index profile $n(r)$ and the group index $N(r)$.
It the following a linear relation between $n(r)$ and $N(r)$ is assumed (fig. 5.7).
For example this relation can be described as:

$$N(r) = \frac{N_1}{n_1} \left[(1 - P) \cdot n(r) + n_1 \cdot P\right] \tag{5.28}$$

The parameter $P$ is called the *profile dispersion parameter*. If eq. (5.28) is true, the parameter is called linear profile dispersion. Thus, $P$ depends only on the wavelength $\lambda$ and not on the radius $r$.
In order to explain the term of the profile dispersion, the relation between $\Delta n$ and $\Delta N$ in fig. 5.7 will be analyzed in details. The refractive index difference $\Delta n$ can be specified as:

$$\Delta n = \frac{n_1 - n_2}{n_1} \cdot n_1 = \Delta \cdot n_1 \qquad \text{mit} \quad \Delta = \frac{n_1 - n_2}{n_1}, \tag{5.29}$$

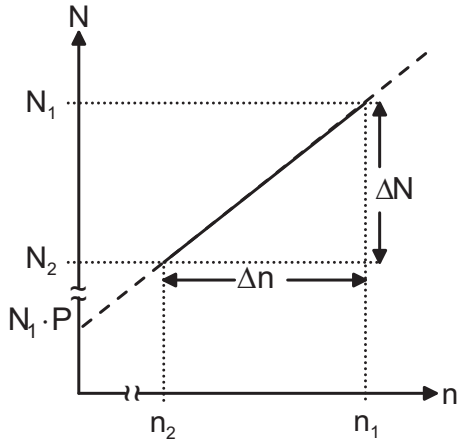


Figure 5.7: Group index $N(r)$ as a function of the refractive index $n(r)$

where $\Delta$ describes the relative refraction index difference between the fiber core and the fiber cladding. In analogy to $N = n - \lambda \frac{\mathrm{d}n}{\mathrm{d}\lambda}$, for the difference between the group index $\Delta N$ applies:

$$\Delta N = \Delta n - \lambda \frac{\mathrm{d}\left(\Delta n\right)}{\mathrm{d}\lambda} \tag{5.30}$$

and therefore

$$\Delta N = \Delta \cdot n_1 - \lambda \frac{\mathrm{d}\left(\Delta \cdot n_1\right)}{\mathrm{d}\lambda} \tag{5.31}$$

$$= \Delta \cdot n_1 - \lambda \cdot \Delta \frac{\mathrm{d}n_1}{\mathrm{d}\lambda} - \lambda \cdot n_1 \frac{\mathrm{d}\Delta}{\mathrm{d}\lambda} \tag{5.32}$$

$$= \Delta \cdot N_1 - \lambda \cdot n_1 \frac{\mathrm{d}\Delta}{\mathrm{d}\lambda} \tag{5.33}$$

On the other hand, eq. (5.28) can be written as:

$$\Delta N = \frac{N_1}{n_1}(1 - P) \cdot \Delta n = \Delta \cdot N_1 \cdot (1 - P) \tag{5.34}$$

which results, after comparison with eq. (5.31), in the profile dispersion of the form:

$$P = \frac{n_1}{N_1} \cdot \frac{\lambda}{\Delta} \cdot \frac{\mathrm{d}\Delta}{\mathrm{d}\lambda} \tag{5.35}$$

Thus, the profile dispersion can be determined by measuring the wavelength dependent numeric aperture (and therefore $\Delta(\lambda)$).

### 5.3.2 Determination of the group delay of the individual eigenmodes

The group propagation delay of a certain eigenmode $(l, p)$ per fiber length $\tau = \mathrm{d}\beta / \mathrm{d}\omega$ is a result of (5.15), if eq. (5.15) is differentiated with respect to $\omega$.

$$\frac{\mathrm{d}}{\mathrm{d}\omega}\left(\int_{r_1}^{r_2} k_r \, \mathrm{d}r\right) = 0 = \int_{r_1}^{r_2} \frac{1}{k_r}\left[k_0 n(r) \frac{\mathrm{d}\left(\omega \cdot n(r)\right)}{c \cdot \mathrm{d}\omega} - \beta \cdot \tau\right] \mathrm{d}r \tag{5.36}$$

In eq. (5.36) the differentiation of $k_r$ with respect to $\omega$ (eq. (5.8)) was used. The relation $k_0 = \omega/c$ was also utilized. Eq. (5.36) can be solved for the desired delay $\tau$:

$$\tau = \frac{k_0}{\beta \cdot c} \frac{\int_{r_1}^{r_2} \frac{1}{k_r} n(r) \cdot N(r) \, \mathrm{d}r}{\int_{r_1}^{r_2} \frac{1}{k_r} \, \mathrm{d}r} \tag{5.37}$$

with the group index $N(r) = \mathrm{d}\left(\omega \cdot n(r)\right) / \mathrm{d}\omega$ taken from the chapter GRU eq. 25.
Firstly, for any arbitrary eigenmode $(l, p)$, the phase constant $\beta$ can be determined from eq. (5.8) and eq. (5.15). Then the group delay $\tau$ can be calculated from eq. (5.37).

The refractive index profile $n(r)$ (and therefore $N(r)$, according to eq. (5.28)), will now be optimized so that every eigenmode has the same propagation delay $\tau$. In this general form, this is a complicated numerical optimization process.
In this case we limit ourselves on the profile class of the so-called potential profiles ("power-law-profiles") (see fig. 5.8), where the refractive index is described by:

$$n^2(r) = \begin{cases} n_1^2 \left(1 - 2\Delta \left(\frac{r}{a}\right)^g\right) & \text{for } r \leq a \\ n_1^2(1 - 2\Delta) = n_2^2 & \text{for } r > a \end{cases} \tag{5.38}$$

with the profile exponent $g$. For example the parabolic refractive index profile is described by $g = 2$ and furthermore the step-index profile is characterized with $g = \infty$. For the refractive index profile according

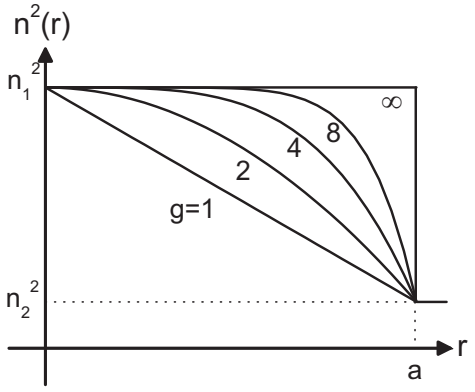


Figure 5.8: Potential profile for different profile exponents $g$

to eq. (5.38) it applies (without proof) that the propagation delay of $\tau$ in eq. (5.37) only depends on $\beta$, but doesn't depend on the circumferential order $l$ (which is in principle contained in $k_r$). Under this condition, in analogy to eq. (5.20) and eq. (5.21), both the numerator and the denominator of eq. (5.37) can be integrated over $l$ without corruption of the result for $\tau$.

After commutation of the integration order (shown in eq. (5.21)) the integration over $l$ can be solved analytically and takes the form:

$$\begin{aligned}\tau = \frac{d\beta}{d\omega} &= \frac{1}{c} \cdot \frac{k_0}{\beta \cdot \frac{r_0^2}{2}} \int_0^{r_0} n(r)N(r)r \,\mathrm{d}r \\ &= \frac{1}{c} \cdot \frac{1}{n(r_0) \cdot \frac{r_0^2}{2}} \int_0^{r_0} n(r)N(r)r \,\mathrm{d}r \mathrel{\hat{=}} \frac{< n(r)N(r) >}{c \cdot n(r_0)}\end{aligned} \tag{5.39}$$

where $r_0$ is given by $\beta = n(r_0)/k_0$ (compare to fig. 5.9). The notation $< ... >$ in this context means the averaging over the fiber cross-section with $r < r_0$ .

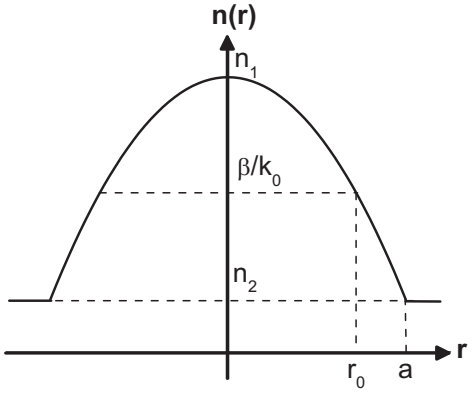


Figure 5.9: Parabolic refraction index profile $n(r)$ and the radius $r_0$

In order to minimize the propagation delay differences between the eigenmodes, a profile optimization of the refractive index profile $n(r)$ has to be determined. To achieve this aim the ration between the numerator and the denumerator in eq. (5.39) should be as independent as possible of $r_0$ and $\beta$, respectively.
For a potential profile as shown in fig. (5.38) and linear profile dispersion (see eq. (5.28)):

$$n(r)N(r) = \frac{N_1}{n_1}\left((1-P)\cdot n^2(r) + n(r)\cdot n_1 \cdot P\right) \approx n_1 N_1 \left(1 - 2\Delta\left(1 - \frac{P}{2}\right)\left(\frac{r}{a}\right)^g\right) \tag{5.40}$$

applies. By using the approximation $n(r_0) \approx n_1\left(1 - \Delta\left(\frac{r_0}{a}\right)^g\right)$, eq. (5.39) can be written as:

$$\tau \approx \frac{1}{c} \cdot \frac{n_1 N_1 \left(1 - 4\Delta\frac{1-\frac{P}{2}}{g+2}\left(\frac{r_0}{a}\right)^g\right)}{n_1\left(1 - \Delta\left(\frac{r_0}{a}\right)^g\right)} \tag{5.41}$$

### 5.3.3 Optimization of the refractive index profile

The propagation delay $\tau$ becomes independent with the approximation in eq. (5.41) of $r_0$ and therefore of $\beta$ for the optimum profile exponent $g = g_{opt}$, with

$$g_{opt} = 2 - 2P \tag{5.42}$$

As a result of the equation above without the approximations for $n(r)$, a more accurate expression for the optimum profile exponent is given by:

$$g_{opt} = 2 - 2P - \Delta\frac{(4-2P)\cdot(3-2P)}{5-4P} \tag{5.43}$$

which differs only slightly from eq. (5.42). Since the profile dispersion parameter $P$ is dependent of the material composition and the wavelength, also the optimum profile exponent $g_{opt}$ is dependent of these variables (see fig. 5.10). For technology reasons mainly the $GeO_2$-doping is used to diversify the refractive index. Thus, there are significant differences for the adjusting profile, whether the fiber should be employed for e.g. $\lambda = 0.8\,\mu m$ or $\lambda = 1.55\,\mu m$. Due to the different delays of the individual modes a pulse broadening

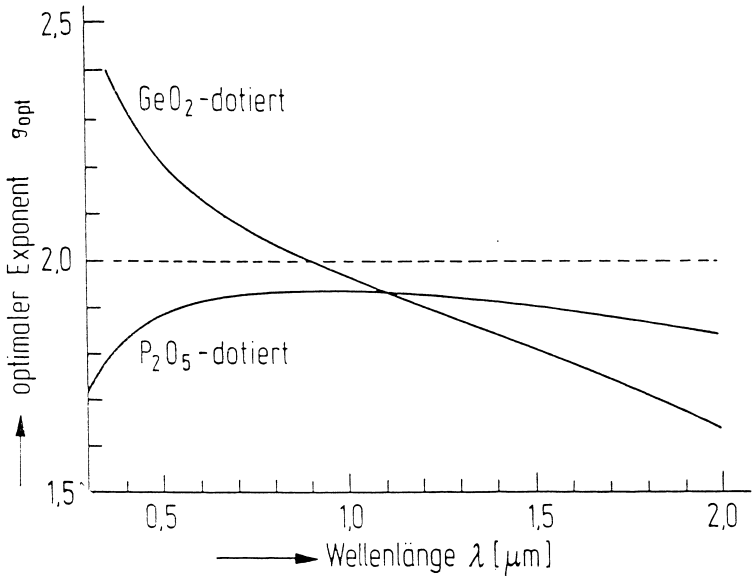


Figure 5.10: Optimized profile exponent $g_{opt}$ for germanium and phosphorus doped silica glass as a function of the wavelength $\lambda$

occurs, which limits the bandwidth. Hence, the bandwidth is:

$$B \sim \frac{1}{(\tau_{max} - \tau_{min})L} \tag{5.44}$$

$\tau_{max}$ and $\tau_{min}$ denote the minimum and maximum delay given by eq. (5.41). From fig. 5.11 the maximum bandwidth of approx. $10\,\text{GHz}\cdot\text{km}$ results for $g = g_{opt}$. If the profile exponent $g$ diverges from the optimal exponent $g_{opt}$, according to fig. 5.11, the result is a minor bandwidth. In practice, the optical fiber manufacturing deviations $|g - g_{opt}| < 0.1$ are manageable, so that bandwidths up to $1\,\text{GHz}\cdot\text{km}$ are still feasible.

In the consideration above, the bandwidth is inversely proportional to the fiber length. In fact, the bandwidth decreases less with increasing fiber length, perhaps in the form

$$B = B_0\left(\frac{L_0}{L}\right)^{\gamma} \qquad \text{mit } \gamma = 0.5...0.8 \tag{5.45}$$

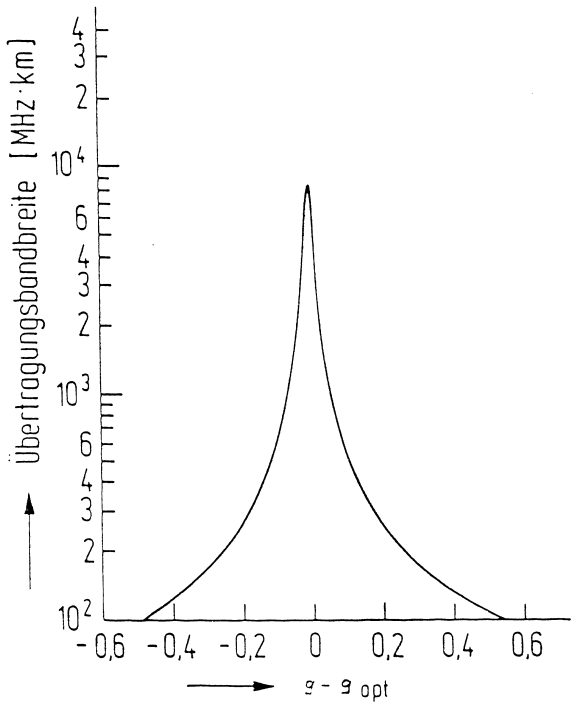


Figure 5.11: 6 dB-Bandwidth of the transmitted electrical signal of a multi-mode graded index with numerical aperture $A_N = 0,24$

$L_0$ is the fiber length to which the bandwidth $B_0$ is related. This may be due to:

1. The refractive index profile is subject to fluctuations, that means fiber pieces alternate between $g - g_{opt} > 0$ and $g - g_{opt} < 0$.

2. According to micro curvature of the fiber, couplings occur between the waves. Hence, fast and slow waves exchange their energy with each other.

A typical dimension for multi-mode graded-index fibers would have, for example, a core diameter of $2a = 50\,\mu\text{m}$, a cladding diameter of $D = 125\,\mu\text{m}$, a numerical aperture $A_N = 0.2$ and a bandwidth of approx. 1 GHz for 1 km fiber length.